Journal of Oceanology and Limnology
Vol. 36 No. 2, P. 341-350, 2018
https://doi.org/10.1007/s00343-018-6281-z

Fish-mediated changes in bacterioplankton community composition: an in situ mesocosm experiment*

LUO Congqiang (罗丛强)[1, 2], YI Chunlong (易春龙)[1], NI Leyi (倪乐意)[1],
GUO Longgen (过龙根)[1, **]

[1] *Donghu Experimental Station of Lake Ecosystems*, *State Key Laboratory of Freshwater Ecology and Biotechnology of China*, *Institute of Hydrobiology*, *Chinese Academy of Sciences*, *Wuhan 430072*, *China*

[2] *Collaborative Innovation Center for Efficient and Health Production of Fisheries in Hunan Province*, *Key Laboratory of Health Aquaculture and Product Processing in Dongting Lake Area of Hunan Province*, *Hunan University of Arts and Science*, *Changde 415000*, *China*

Received Oct. 11, 2016; accepted in principle Jan. 4, 2017; accepted for publication Feb. 10, 2017

Abstract We characterized variations in bacterioplankton community composition (BCC) in mesocosms subject to three different treatments. Two groups contained fish (group one: *Cyprinus carpio*; group two: *Hypophthalmichthys molitrix*); and group three, the untreated mesocosm, was the control. Samples were taken seven times over a 49-d period, and BCC was analyzed by PCR-denaturing gradient gel electrophoresis (DGGE) and real-time quantitative PCR (qPCR). Results revealed that introduction of *C. carpio* and *H. molitrix* had a remarkable impact on the composition of bacterioplankton communities, and the BCC was significantly different between each treatment. Sequencing of DGGE bands revealed that the bacterioplankton community in the different treatment groups was consistent at a taxonomic level, but differed in its abundance. *H. molitrix* promoted the richness of Alphaproteobacteria and Actinobacteria, while more bands affiliated to Cyanobacteria were detected in *C. carpio* mesocosms. The redundancy analysis (RDA) result demonstrated that the BCC was closely related to the bottom-up (total phosphorus, chlorophyll a, phytoplankton biomass) and top-down forces (biomass of copepods and cladocera) in *C. carpio* and control mesocosms, respectively. We found no evidence for top-down regulation of BCC by zooplankton in *H. molitrix* mesocosms, while grazing by protozoa (heterotrophic nanoflagellates, ciliates) became the major way to regulate BCC. Total bacterioplankton abundances were significantly higher in *C. carpio* mesocosms because of high nutrient concentration and suspended solids. Our study provided insights into the relationship between fish and bacterioplankton at species level, leading to a deep understanding of the function of the microbial loop and the aquatic ecosystem.

Keyword: bacterioplankton community composition (BCC); PCR-DGGE; qPCR; analysis of similarities (ANOSIM); redundancy analysis (RDA)

1 INTRODUCTION

Bacterioplankton play a crucial part in energy flow, nutrient cycling and secondary metabolism in aquatic ecosystems (Cole et al., 1988). They are grazed by most protozoa and some metazooplankton and so are tightly linked into the grazing food chain. Since the development of the concept of the "microbial loop", substantial research has been devoted to evaluating the factors regulating bacterioplankton community composition (BCC) (Jürgens and Jeppesen, 2000; Kisand and Zingel, 2000; Zöllner et al., 2003; Niu et al., 2011; Lindh et al., 2015). Top-down (predation) and bottom-up (resources) have been shown to determine bacterioplankton populations. Heterotrophic nanoflagellates (HNF), ciliates and *Daphnia* are the main predators of bacterioplankton in aquatic

* Supported by the National Key Technology R&D Program of China (No. 2014BAC09B02) and the National Water Pollution Control and Management Technology Major Projects (No. 2012ZX07101-002), and the High-Level Scientific Research Foundation for the Introduction of Talent (No. E07016043)
** Corresponding author: longgen@ihb.ac.cn

ecosystems (Jürgens and Jeppesen, 2000; Kisand and Zingel, 2000). Trophic cascades from metazooplankton to bacterioplankton, via phagotrophic protozoans, have also been reported (Zöllner et al., 2003). Bottom-up forces, such as temperature and organic substrates, may also regulate bacterial growth (Niu et al., 2011; Lindh et al., 2015). Organic matter produced by phytoplankton is the key carbon source for bacterioplankton (Baines and Pace, 1991). Under oligotrophic conditions, inorganic nutrients such as phosphorus or nitrogen can limit bacterial growth (Chrzanowski et al., 1995), and phenotypic variations in bacteria have been observed under conditions of different inorganic nutrients (Holmquist and Kjelleberg, 1993; Niu et al., 2015). The existence of close relationships has been shown between the top-down and/or bottom-up factors and BCC. However, there is considerably less information about the extent of potential forces that change the top-down or bottom-up factors, and their indirect effect on bacterioplankton communities.

In this study, we carried out a mesocosm experiment to investigate how the introduction of *Hypophthalmichthys molitrix* and *Cyprinus carpio* modulate the structures of bacterioplankton communities. The introduction of both species into water columns exerts both bottom-up and top-down forces (do Rêgo Monteiro Starling, 1993; Mátyás et al., 2003; Roozen et al., 2007), which probably directly or indirectly affect other trophic components including, of course, the bacterioplankton communities. We hypothesized that *H. molitrix* affects BCC mainly by top-down controls through the grazing food chain. In aquatic ecosystems, *H. molitrix* can significantly reduce the biomass of zooplankton via their filtering mechanisms (do Rêgo Monteiro Starling, 1993; Mátyás et al., 2003). The corresponding predation pressure on protozoa from zooplankton would be relieved if the abundance of zooplankton was considerably decreased (Jürgens and Matz, 2002). Therefore, protozoa (HNF, ciliates) abundance and grazing pressure on bacterioplankton would be enhanced, resulting in morphological changes in the bacterioplankton assemblage. The abundance of grazing-resistant bacterioplankton morphotypes (aggregates, filaments) would increase and the composition of bacterioplankton communities would change accordingly. After the application of molecular methods, such as DGGE and FISH, it could be shown that grazing-resistant bacterioplankton appeared within the major groups: Alphaproteobacteria, Betaproteobacteria and Cytophaga-Flavobacteria (Jürgens et al., 1999). We hypothesize that bottom-up controls of *C. carpio* on BCC was the major ways. The selective omnivorous fish, *C. carpio*, generally increase phytoplankton biomass and nutrient concentrations in water bodies via excretion, release of sediment nutrients and resuspension of bottomed phytoplankton cells (Roozen et al., 2007).

To verify these hypotheses, the variations in BCC and bacterioplankton abundance were detected by PCR-denaturing gradient gel electrophoresis (DGGE) and real-time quantitative PCR (qPCR), taking seven samples over a period of 49 days. Redundancy analysis (RDA) was used to identify the major environmental factors acting on BCC. We hypothesized that bacterioplankton would exhibit pronounced treatment differences both in composition and in abundance; that the differences in BCC would largely be explained by changes in biotic and abiotic factors; and that the mechanisms influencing BCC driven by *H. molitrix* and *C. carpio* would be species specific.

2 MATERIAL AND METHOD

2.1 Experiment design

The experiment was carried out in Erhai Lake (25°52′N, 100°06′E), a subtropical lake in the Yunnan Plateau, China (mean depth 10.5 m, maximum depth 20.5 m, area 249.8 km^2). We set up nine independent cylindrical mesocosms (3 m in diameter, 4 m in height) made of waterproof polyvinyl chloride (PVC) textile (Fig.1). The water in the mesocosms was completely isolated from the outer water environment through the use of mechanical devices, while the upper and lower regions of the mesocosms were in direct contact with the air and sediment. Before the start of the experiment, the external and internal water of the mesocosms was fully exchanged, and all fishes were removed.

The nine mesocosms were randomly divided into three groups. In groups one and two, 1-year-old *C. carpio* and *H. molitrix* (with biomass of 50 g/m^3) were introduced, respectively. Group three, without any further processing, was used as the control.

2.2 Sampling and measuring experimental parameters

The experiment was performed from 24 September 2014 to 6 November 2014. Samples were collected on

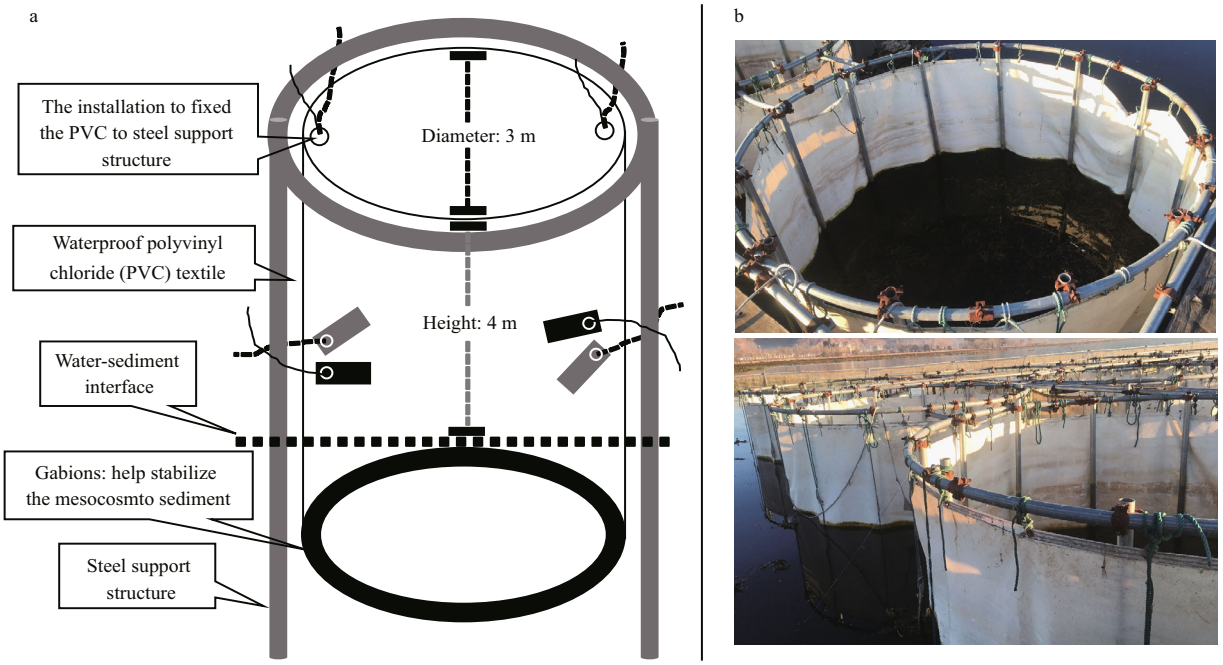

Fig.1 Diagram of design (a) and photographs (b) of mesocosms in place

days 7, 14, 21, 28, 35, 42, and 49 after the introduction of *C. carpio* and *H. molitrix* on day 0. Water samples were collected from the surface (0–0.5 m) with a 5-L Schindler sampler. For phytoplankton identification and counts, 1-L water sample was preserved with 1% Lugol's iodine solution. Zooplankton were collected by filtering 10 L water sample through a 64-μm plankton net and were then preserved with formalin. Water environmental parameters such as temperature (*T*), oxidation-reduction potential, conductivity, dissolved oxygen (DO), total dissolved solids and pH were measured using an YSI Pro Plus (YSI Inc., Yellow Springs, OH, USA) water quality monitor. Chemical parameters including total nitrogen (TN), ammonia nitrogen (NH_4-N), nitrate nitrogen (NO_3-N), phosphate phosphorous (PO_4-P), total phosphorous and chlorophyll *a* (Chl *a*) were determined based on previous references (Greenberg et al., 1992). For bacterioplankton community analysis, a 300-mL water sample was filtered through a 0.2-mm filter membrane (Whatman, 111106, UK). Filters were stored at -80°C until analysis.

2.3 PCR-DGGE fingerprinting

Bacterioplankton genomic DNA was isolated using a water bacterial DNA extraction kit (Omega, D5525-01, USA) following the standard protocols. A Nanodrop ND-1000 spectrophotometer (NanoDrop Technology, USA) was then used to check the purity and concentrations of DNA. Subsequent analysis was conducted on mixtures of DNA, which contained equivalent amounts of DNA from each repetition. DNA fragments of about 200 bp were amplified with bacteria-specific primers 341*F* (5′-CCTACGGGAGGCAGCAG-3′) with a 40-bp GC clamp attached to its 5′ end and the 518*R* (5′-ATTACCGCGGCTGCTGG-3′) primer, as described in Muyzer et al. (1993). Next, 1.5% agarose gel electrophoresis was conducted to confirm the PCR products. A Dcode system (Bio-Rad Laboratories, USA) was used for running the DGGE profiles with a denaturing gradient from 40% to 55%, following the procedure described in Niu et al. (2011). After electrophoresis, the gels were stained with 1:1 000 diluted GelRed (Biotium, 10202ES76, USA) nucleic acid staining solutions for 25 min, and then photographed by use of a Bio Image System (Gene Com.) under UV light. All visible bands were excised, cloned and sequenced for further analysis.

2.4 Real-time quantitative PCR and standard curve

In this study, 16S rRNA gene copy numbers were used as a proxy of bacterioplankton abundance. The PCR method was applied to all DNA samples with the general primers 341*F* (5′-CCTACGGGAGGCAGCAG-3′) and 518*R* (5′-ATTACCGCGGCTGCTGG-3′). The 50 μL PCR mixture contained 0.5 μL of the primer set (25 pmol each), 25 μL PCR premixture (Takara, R004Q, Japan), 1 μL DNA template (40 ng), and 23 μL sterile water. PCR was conducted with the

following thermal cycles: 94°C for 10 min, followed by 33 cycles of 94°C for 10 s, 65°C for 25 s and 72°C for 35 s, and then 72°C for 10 min. The purified PCR products were inserted into the pMD19-T Vector (TaKaRa, 6013, Japan) and transformed into *Escherichia coli* JM109 Electro-Cells (TaKaRa, 9022, Japan). The recombinant plasmid was then extracted using the GenElute™ Plasmid Miniprep Kit (Sigma, PLN70, USA) and the concentrations were detected with a Nanodrop ND-1000 spectrophotometer (NanoDrop Technology, USA). The plasmid DNA copy numbers were calculated according to the concentration of extracted plasmids and its weight, according to the method described in previous references (Li et al., 2009; Wang et al., 2015). A tenfold serial dilution of plasmid DNA from 10^3 to 10^9 copies was used as a standard template in each PCR process. Reasonable amplification efficiency obtained in the experiments should be between 90% and 110%.

Quantitative PCR (qPCR) was performed with the step one plus™ Real-time PCR-system (Applied Biosystems). qPCR amplification was run in triplicate on eight PCR tubes (Axygen, PCR-0208-C, USA). The 25 μL PCR mixture containing 0.5 μL of the primer set (12.5 pmol each), 12.5 μL 1×SYBR Green real-time PCR premixture (Toyobo, QPS-101B, Japan), 3 μL DNA template (40 ng), and 8.5 μL sterile water. The qPCR amplification program was: 94°C for 8 min, followed by 40 cycles of 94°C for 10 s; 65°C for 60 s, 72°C for 35 s, and then 72°C for 10 min. Amplification specificity was evaluated according to the melting curve, which was obtained from 60°C to 95°C at 0.5°C internals after amplification.

2.5 Statistical analysis

DGGE profiles were analyzed using Quantity One software (Version 4.5, Bio-Rad). The values 1 and 0, which corresponded to the presence and absence of the bands in the DGGE profiles, were used to construct binary matrices. Pairwise similarities between samples were quantified using the Dice similarity coefficient (S_D). Values of S_D were then used to construct a dendrogram with the NTSYS Program (version 2.10e, Exeter software, Setauket, NY, USA), based on the unweighted pair-group method with arithmetic averages (UPGMA). Non-parametric permutation procedure analysis of similarities (ANOSIM) was used to test whether BCC between the three treatments was significantly different or not. The time decay of phylogenetic similarity of a bacterioplankton community was applied to assess the temporal turnover of the BCC, using the method described in Chen et al. (2016).

To explore the relationship between BCC and environmental factors (TN, total phosphorus (TP), water temperature, pH, copepod and cladocera biomass, and different phytoplankton taxonomic groups), RDA was performed with the software Canoco for Windows (version 4.5, Microcomputer Power, Ithaca, New York, USA). The significance of the relationships between BCC and environmental factors was determined using Monte Carlo permutation tests. The physical and chemical parameters were subject to one-way analysis of variance (ANOVA) followed by a post hoc comparison test (LSD) with SPSS software (Version 17.0 for Windows, Chicago, IL, USA). Significance was determined at an alpha level of 0.05 (P<0.05).

3 RESULT

3.1 Variations in environmental parameters and bacterioplankton abundance

TN, TP, Chl *a* and phytoplankton biomass were significantly higher (P<0.05) in the *C. carpio* mesocosms than in other treatments (Table 1). There was little variation in abiotic factors between *H. molitrix* and control mesocosms. The biomass of copepods and cladocera were significantly lower in *H. molitrix* mesocosms, and no significant difference was observed in the biomass and structure of zooplankton between *C. carpio* and control mesocosms. For total bacterioplankton abundance, the highest copy number of 16S rDNA was detected in the *C. carpio* mesocosms with an average value of $(3.62\pm1.02)\times10^{11}$/L, and there was no difference in the 16S rDNA copy number between *H. molitrix* and control mesocosms.

3.2 BCC

DGGE was used to examine the bacterioplankton community feature in 21 samples (seven samples for each treatment) (Fig.2); 51 distinct bands were excised from the DGGE gels, and 26–36 bands were detected per sample. As shown by UPGMA (Fig.3) and ANOSIM (Table 2), each treatment maintained complex and specific bacterioplankton communities. The cluster (UPGMA) analysis showed that all the samples were clustered into three distinct groups, and the samples obtained from each single treatment were clustered together. ANOSIM confirmed that the variation in BCC was higher among treatments than

Table 1 Physico-chemical and biological parameters, and the abundance of copy number of 16S rDNA in different treatment groups from 24 September to 6 November 2014

Treatment	*C. carpio* (*n*=3)	*H. molitrix* (*n*=3)	Control (*n*=3)
Total nitrogen (TN, mg/L)	2.01±0.82[a]	1.24±0.64[b]	1.21±0.31[b]
Total phosphorus (TP, mg/L)	0.14±0.08[a]	0.07±0.02[b]	0.06±0.02[b]
Total dissolved nitrogen (TDN, mg/L)	0.72±0.34[a]	0.51±0.12[a]	0.51±0.22[a]
Total dissolved phosphorus (TDP, mg/L)	0.029±0.013[a]	0.027±0.009[a]	0.023±0.012[a]
NH_4-N (mg/L)	0.074±0.023[a]	0.068±0.009[a]	0.012±0.008[b]
NO_3-N (mg/L)	0.13±0.06[a]	0.13±0.05[a]	0.12±0.03[a]
Conductivity (S/cm)	388±24[a]	367±51[a]	368±56[a]
Dissolved oxygen (DO, mg/L)	7.73±2.13[a]	7.56±1.53[a]	9.93±2.54[b]
Chlorophyll *a* (Chl *a*, μg/L)	172.10±32.56[a]	50.24±12.74[b]	46.62±13.71[b]
pH	8.15±0.54[a]	8.23±0.83[a]	8.25±0.39[a]
Phytoplankton biomass (mg/L)	5.33±1.28[a]	0.95±0.26[b]	1.05±0.18[b]
Copepods biomass (mg/L)	0.89±0.21[a]	0.01±0.002[b]	0.95±0.23[a]
Cladocera biomass (mg/L)	0.80±0.16[a]	0.01±0.005[b]	0.89±0.12[a]
Copy number of 16S rDNA (copies/L)	(3.62±1.02)×10^{11a}	(8.95±2.13)×10^{9b}	(5.21±1.68)×10^{9b}

Analysis of variance (ANOVA) was used to examine differences among the parameters of the three treatments. Different lower-case letters indicate significant differences among the treatments. Data represent mean±SD.

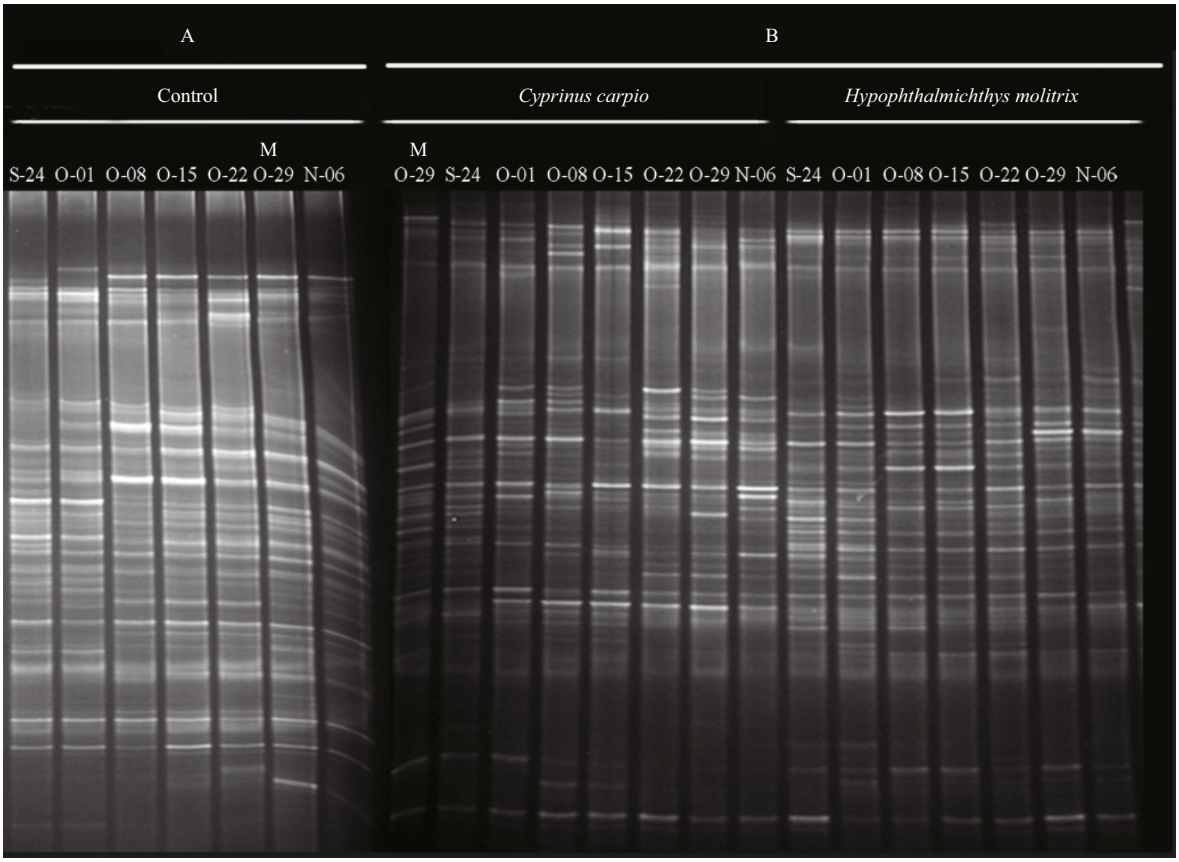

Fig.2 PCR-denaturing gradient gel electrophoresis (DGGE) profiles of 16S rRNA gene fragments from different treatment groups from 24 September to 6 November 2014

The letter M, as shown in the figure, was used as Marker in DGGE profiles A and B

within treatments (R>0.612; P>0.01). In addition, similarity values between two lanes showed discrepancies between treatments.

Assessments of the temporal turnover rate of BCC in the time-similarity relationship for *C. carpio*, *H. molitrix* and control treatments are presented in

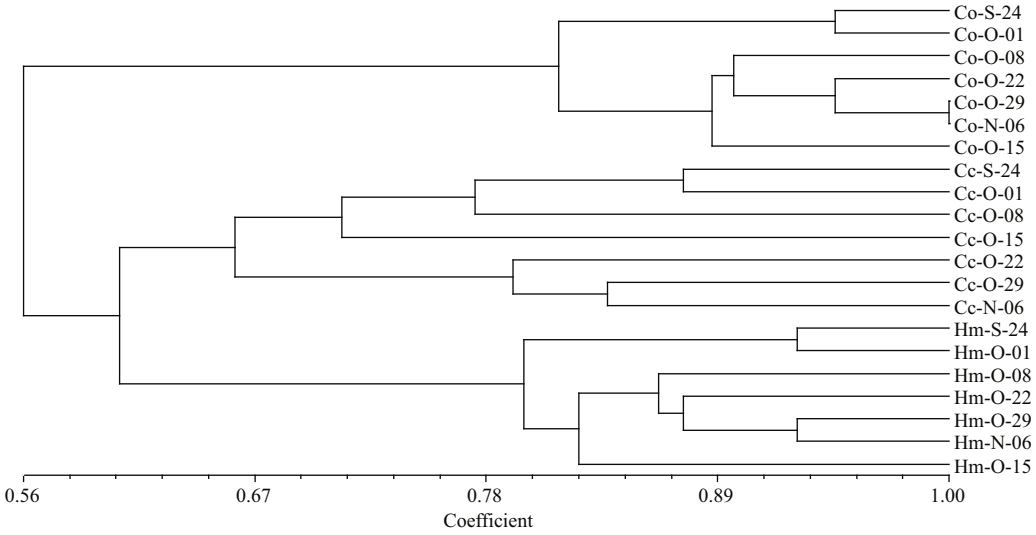

Fig.3 Cluster analysis of bacterioplankton communities based on PCR-denaturing gradient gel electrophoresis (DGGE) profiles from the different treatment groups

Cc, Hm, and Co represent samples from *Cyprinus carpio*, *Hypophthalmichthys molitrix* and control mesocosms, respectively.

Table 2 Analysis of similarity (ANOSIM) for the comparison of PCR-denaturing gradient gel electrophoresis (DGGE) profiles of bacterioplankton community structure among different treatments

Comparison			R^a	P^b
C. carpio	vs	*H. molitrix*	0.612	0.001
C. carpio	vs	Control	0.8	0.002
H. molitrix	vs	Control	1	0.001

[a]*R* values close to 1 suggest dissimilarity of samples groups; >0.75 means well separated; >0.5 means separated but overlapping; <0.25 means barely separable; close to 0 means no separation. [b] Differences are considered significant at $P<0.05$.

Fig.4. Significant time decay model for similarity of the BCC were well detected across all treatments ($P<0.001$), with turnover rates of 0.150, 0.149 and 0.091 at the *C. carpio*, *H. molitrix* and control mesocosms, respectively. A permutation test ($P<0.001$) showed that all turnover rates significantly deviated from 0. The rate of *C. carpio* and *H. molitrix* mesocosm samples was significantly higher than samples in the control mesocosms, indicating that the introduction of *C. carpio* and *H. molitrix* accelerated the temporal turnover of BCC.

3.3 Phylogenetic analysis of sequenced DGGE bands

From the DGGE profiles, 51 bands from different positions were successfully sequenced. These sequences were compared using the classifier tool in RDP and their taxonomic information is shown in Table S1. The majority of bacterioplankton detected from the three treatments were the same, and were affiliated to the groups Bacteroidetes, Alphaproteobacteria, Cyanobacteria, and Actinobacteria. Sequences belonging to Gammaproteobacteria, Betaproteobacteria (5.9%), Firmicutes, and Thermoprotei were also detected at low numbers.

It has been demonstrated that band intensity in gel profiles corresponds to the relative abundance of phylotypes in the DNA template mixture; the higher intensity band was assumed to be dominant (Fromin et al., 2002). Thus, phylotype richness differed between the treatment groups, both in the presence of distinct bands and differences in the intensity of ubiquitous bands (Table S1). The introduction of *C. carpio* led to an increase in the number of bands belonging to Cyanobacteria: among them, three bands (EH-Clones-1, 6, 15) were unique. All the Alphaproteobacteria detected in our study appeared in, and dominated, *H. molitrix* mesocosms.

3.4 Nucleotide sequence accession numbers

The 16S rRNA gene sequences have been deposited to NCBI under Accession Nos. KT864877–KT864925.

3.5 Relationships between BCC and environmental variables

Based on RDA analysis (Fig.5), variation in BCC was best explained by bottom-up factors (TN, TP, Chl *a* and the phytoplankton biomass) as well as by top-down factors (copepod and cladocera biomass). These investigated environmental factors explained 35.4% of the total variance in BCC in all samples

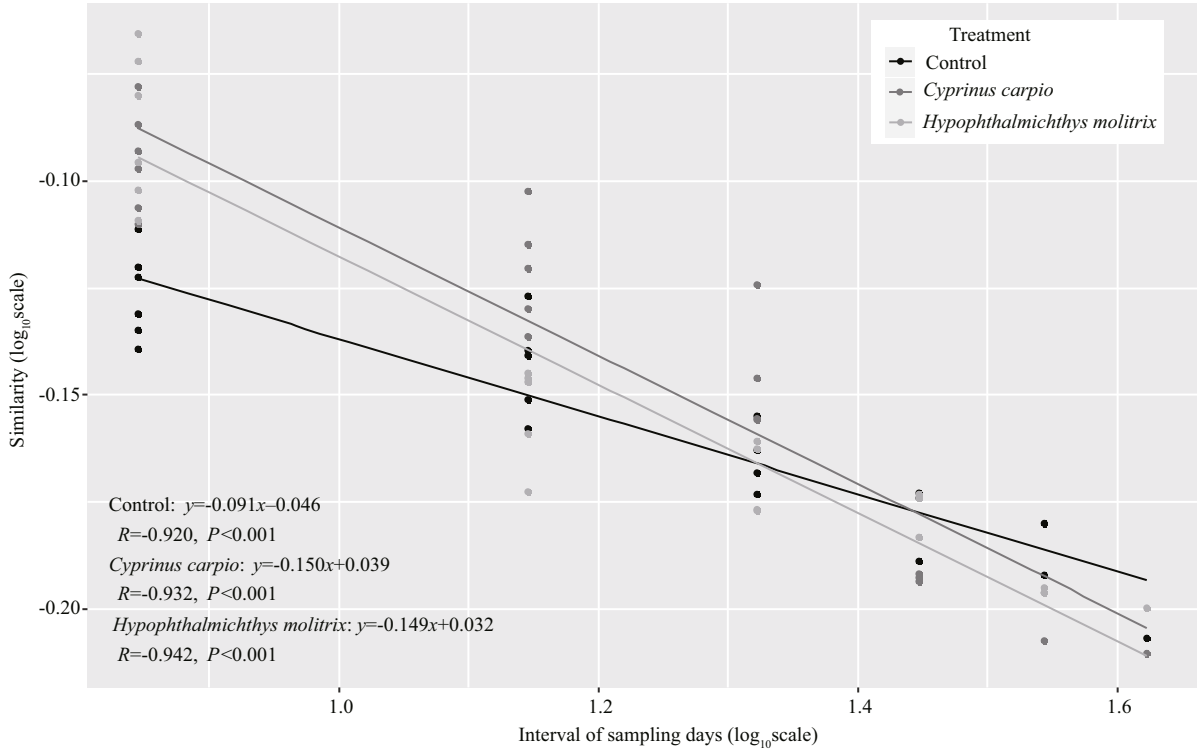

Fig.4 Time-decay models of similarity of bacterioplankton community composition in three treatments

The data for similarity value and days between detection are shown as $\log_{10}$ transformed.

based on the first two axes. In *C. carpio* mesocosms, TP, Chl *a* and phytoplankton biomass significantly explained the variation in BCC. In control mesocosms, cladocera and copepod biomass was significantly related to BCC, while in *H. molitrix* mesocosms the correlations between BCC and those factors were weak.

4 DISCUSSION

Consistent with our original expectations, an alteration in high trophic level organisms was apparent at the bacterial level in aquatic ecosystems. In this study, the DGGE banding patterns and subsequent statistical (ANOSIM and UMGMA) analyses revealed that BCC was significantly different among treatment groups, indicating that the addition of *C. carpio* and *H. molitrix* produced different influences on the BCC. Introduction of *C. carpio* and *H. molitrix* increased the number of 16S rRNA gene copies, especially in the *C. carpio* mesocosms. Those results were in line with previous studies, which showed fish were the important driving force for the change in BCC in aquatic ecosystems (Saarenheimo et al., 2016). RDA results revealed several significant relationships between BCC and explanatory variables. Bottom-up (TP, Chl *a* and phytoplankton biomass) and top-down factors

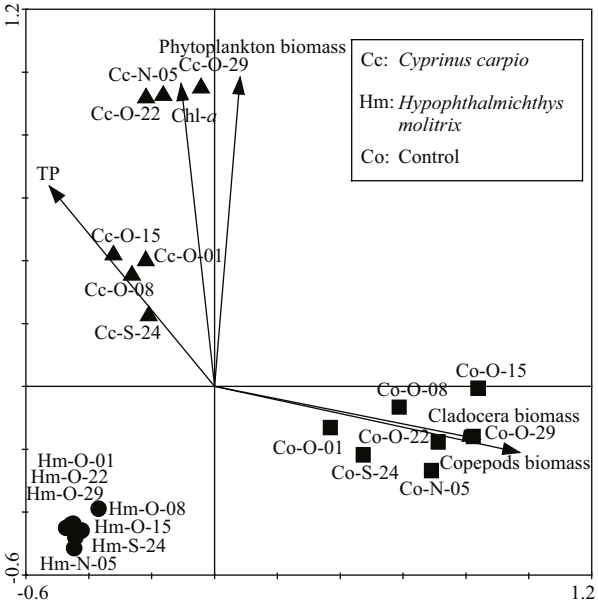

Fig.5 Redundancy analysis (RDA) biplots showing bacterioplankton communities from different treatment samples in relation to environmental factors

(copepod and cladocera biomass) were found to be closely related to changes in the bacterioplankton communities in the three treatments studied, and the relationship between explanatory variables and BCC differed according to the treatments.

In mesocosms with *C. carpio*, the bottom-up forces, including phytoplankton biomass, Chl *a*, and TP, more or less explained the variation in BCC. All three parameters were higher in *C. carpio* mesocosms than in the other treatments; this agrees with research showing that *C. carpio* can enhance these factors via excretion and bioturbation (Roozen et al., 2007). It is well known that phytoplankton have crucial roles in regulating bacterioplankton in natural or mesocosm systems (Pinhassi et al., 2004; Niu et al., 2011). Co-variation between specific bacterioplankton taxa and various phytoplankton taxonomic groups have also been observed (Pinhassi et al., 2004). These tight correlations between bacterioplankton communities and phytoplankton are due to the importance of dissolved organic matter released by phytoplankton and which provides a source of carbon for bacterioplankton (Baines and Pace, 1991). Inorganic nutrients can directly affect the BCC as well as the bacterioplankton through effects on growth (Chrzanowski et al., 1995). The clear relationship between BCC and nutrients also originates from the co-variation in nutrients with phytoplankton (Baines and Pace, 1991), since phytoplankton can use these dissolved inorganic nutrients to reproduce and therefore influence the bacterioplankton communities via release of organic carbon to the water column. In the three treatment groups, the values of dissolved phosphorus and nitrogen concentrations did not drop below 10 μmol/L in any samples, which is an important threshold beneath which bacterial growth is restricted (Chrzanowski et al., 1995). Therefore, the relationship between high nutrients and BCC in *C. carpio* mesocosms is probably indirect, and mediated by the abundance of phytoplankton.

The RDA results in the present study do not signify that top-down control has no effect on BCC in *H. molitrix* mesocosms. From our results, we can only conclude that there was no direct predation pressure on the bacterioplankton by zooplankton in *H. molitrix* mesocosms for its lower biomass. However, the top-down control on bacterioplankton communities by protozoa (e.g. NHF, ciliates) improves in *H. molitrix* mesocosms, because a low abundance of zooplankton exerts low predation pressure on protozoans. Previous studies showed that there was an obvious change in the BCC when zooplankton populations were removed, and generally tend toward increasing the rate of grazing-resistant bacteria (Langenheder and Jürgens, 2001; Jürgens and Matz, 2002). DNA-fingerprinting methods such as PCR-DGGE also revealed that these grazing-resistant bacteria mainly belonged to the subdivisions Alphaproteobacteria, Betaproteobacteria and Bacteroidetes (Jürgens et al., 1999), and a high abundance of Alphaproteobacteria was found in mesocosms with *H. molitrix*. Although we did not include protozoan (e.g. NHF, ciliates) communities in our study, on combining the above results, we believe that top-down control by protozoans would be an important factor in the regulation of BCC in *H. molitrix* mesocosms.

Cyprinus carpio and *H. molitrix* might also make a direct contribution to BCC succession. We believe that the digestive tracts of fish could be seen as a screening tool for bacteria, particularly in filter-feeding fish, with only the species that can survive the gut environment being released into the water column. In addition, the allochthonous and sediment bacteria were also the main source for aquatic ecosystem (Wu et al., 2007). Therefore, we speculate that *C. carpio* would affect BCC via the resuspension of bacteria from the sediment.

Analysis of DGGE band sequences demonstrates that the number and richness of the dominant taxa differed among treatment groups, suggesting that *C. carpio* and *H. molitrix* not only influence the structure of the bacterioplankton community, but may also change the bacterioplankton at the taxonomic level. For example, the highest numbers of Cyanobacteria were observed in *C. carpio* mesocosms, and four of them were typical of this environment, suggesting that the Cyanobacteria have competitive advantages over other bacterioplankton in water columns with *C. carpio*. Introduction of *H. molitrix* can increase the abundance of Alphaproteobacteria. Since it has been reported that there are many species in aquatic ecosystems, it is possible that particular species—perhaps sensitive to environmental changes after the introduction of *H. molitrix* and *C. carpio*—might have been overlooked by our methods. With advanced methods such as second-generation sequencing, it may be possible to present the systematic variations in BCC that can be ascribed to particular species of fish.

5 CONCLUSION

This study demonstrated that *C. carpio* and *H. molitrix* were important structuring forces on BCC, and that the influencing mechanism is species specific. In *H. molitrix* mesocosms, the biomass of zooplankton was low and resulted in weak cascading effects on BCC. According to sequencing results, the effect of

top-down control by protozoan (e.g. NHF, ciliates) grazers is apparently the main reason for the change in BCC. In *C. carpio* mesocosms, bottom-up effects of high nutrient concentrations (TN, TP, etc.) on BCC were not clearly detected, but which cooperation with phytoplankton biomass to influence BCC. These results further our understanding of the changes in BCC in freshwater ecosystems after the introduction of *C. carpio* and *H. molitrix*, and so are especially significant in guiding aquaculture management.

References

Baines S B, Pace M L. 1991. The production of dissolved organic matter by phytoplankton and its importance to bacteria: patterns across marine and freshwater systems. *Limnol. Oceangr.*, **36**(6): 1 078-1 090.

Chen X X, Wang K, Guo A N, Dong Z Y, Zhao Q F, Qian J, Zhang D M. 2016. Excess phosphate loading shifts bacterioplankton community composition in oligotrophic coastal water microcosms over time. *J. Exp. Mar. Biol. Ecol.*, **483**: 139-146.

Chrzanowski T H, Sterner R W, Elser J J. 1995. Nutrient enrichment and nutrient regeneration stimulate bacterioplankton growth. *Microb. Ecol.*, **29**(3): 221-230.

Cole J J, Findlay S, Pace M L. 1988. Bacterial production in fresh and saltwater ecosystems: a cross-system overview. *Mar. Ecol. Prog. Ser.*, **43**: 1-10.

do Rêgo Monteiro Starling F L. 1993. Control of eutrophication by silver carp (*Hypophthalmichthys molitrix*) in the tropical Paranoá Reservoir (Brasília, Brazil): a mesocosm experiment. *Hydrobiologia*, **257**(3): 143-152.

Fromin N, Hamelin J, Tarnawski S, Roesti D, Jourdain-Miserez K, Forestier N, Teyssier-Cuvelle S, Gillet F, Aragno M, Rossi P. 2002. Statistical analysis of denaturing gel electrophoresis (DGE) fingerprinting patterns. *Environ. Microbiol.*, **4**(11): 634-643.

Greenberg A E, Clesceri L S, Eaton A D. 1992. Standard Methods for the Examination of Water and Wastewater. 18th edn. American Public Health Association, Washington D.C.

Holmquist L, Kjelleberg S. 1993. Changes in viability, respiratory activity and morphology of the marine *Vibrio* sp. strain S14 during starvation of individual nutrients and subsequent recovery. *FEMS Microbiol. Ecol.*, **12**(4): 215-223.

Jürgens K, Jeppesen E. 2000. The impact of metazooplankton on the structure of the microbial food web in a shallow, hypertrophic lake. *J. Plankton Res.*, **22**(6): 1 047-1 070.

Jürgens K, Matz C. 2002. Predation as a shaping force for the phenotypic and genotypic composition of planktonic bacteria. *Antonie van Leeuwenhoek*, **81**(1-4): 413-434.

Jürgens K, Pernthaler J, Schalla S, Amann R. 1999. Morphological and compositional changes in a planktonic bacterial community in response to enhanced protozoan grazing. *Appl. Environ. Microbiol.*, **65**(3): 1 241-1 250.

Kisand V, Zingel P. 2000. Dominance of ciliate grazing on bacteria during spring in a shallow eutrophic lake. *Aquat. Microb. Ecol.*, **22**(2): 135-142.

Langenheder S, Jürgens K. 2001. Regulation of bacterial biomass and community structure by metazoan and protozoan predation. *Limnol. Oceanogr.*, **46**(1): 121-134.

Li M, Penner G B, Hernandez-Sanabria E, Oba M, Guan L L. 2009. Effects of sampling location and time, and host animal on assessment of bacterial diversity and fermentation parameters in the bovine rumen. *J. Appl. Microbiol.*, **107**(6): 1 924-1 934.

Lindh M V, Lefébure R, Degerman R, Lundin D, Andersson A, Pinhassi J. 2015. Consequences of increased terrestrial dissolved organic matter and temperature on bacterioplankton community composition during a Baltic Sea mesocosm experiment. *AMBIO*, **44**(S3): 402-412.

Mátyás K, Oldal I, Korponai J, Tátrai I, Paulovits G. 2003. Indirect effect of different fish communities on nutrient chlorophyll relationship in shallow hypertrophic water quality reservoirs. *Hydrobiologia*, **504**(1-3): 231-239.

Muyzer G, de Waal E C, Uitterlinden A G. 1993. Profiling of complex microbial populations by denaturing gradient gel electrophoresis analysis of polymerase chain reaction-amplified genes coding for 16S rRNA. *Appl. Environ. Microbiol.*, **59**(3): 695-700.

Niu Y, Shen H, Chen J, Xie P, Yang X, Tao M, Ma Z M, Qi M. 2011. Phytoplankton community succession shaping bacterioplankton community composition in Lake Taihu, China. *Water Res.*, **45**(14): 4 169-4 182.

Niu Y, Yu H, Jiang X. 2015. Within-lake heterogeneity of environmental factors structuring bacterial community composition in Lake Dongting, China. *World J. Microbiol. Biotechnol.*, **31**(11): 1 683-1 689.

Pinhassi J, Sala M M, Havskum H, Peters F, Guadayol Ò, Malits A, Marrasé C. 2004. Changes in bacterioplankton composition under different phytoplankton regimens. *Appl. Environ. Microbiol.*, **70**(11): 6 753-6 766.

Roozen F C J M, Lürling M, Vlek H, Van Der Pouw Kraan E A J, Ibelings B W, Scheffer M. 2007. Resuspension of algal cells by benthivorous fish boosts phytoplankton biomass and alters community structure in shallow lakes. *Freshwater Biol.*, **52**(6): 977-987.

Saarenheimo J, Aalto S L, Syväranta J, Devlin S P, Tiirola M, Jones R I. 2016. Bacterial community response to changes in a tri-trophic cascade during a whole-lake fish manipulation. *Ecology*, **97**(3): 684-693.

Wang S Q, Zhu L, Li Q, Li G B, Li L, Song L R, Gan N Q. 2015. Distribution and population dynamics of potential anatoxin-a-producing cyanobacteria in Lake Dianchi, China. *Harmful Algae*, **48**: 63-68.

Wu Q L, Zwart G, Wu J F, Kamst-van Agterveld M P, Liu S J, Hahn M W. 2007. Submersed macrophytes play a key role in structuring bacterioplankton community composition in the large, shallow, subtropical Taihu Lake, China. *Environ. Microbiol.*, **9**(11): 2 765-2 774.

Zöllner E, Santer B, Boersma M, Hoppe H G, Jürgens K. 2003. Cascading predation effects of *Daphnia* and copepods on microbial food web components. *Freshwater Biol.*, **48**(12): 2 174-2 193.

Table S1 Taxonomic descriptions of the 51 bands excised from the DGGE gels of the three different treatment groups

Band	Accession No.	Habitat[a]	Taxon	Closest relative
EH-Clone-1	KT864877	**Cc**	Cyanobacteria	*Aphanizomenon aphanizomenoides* 22C4.9 (EF529479)
EH-Clone-2	KT864878	**Cc**	Bacteroidetes	Uncultured bacterium clone B0618R003_D20 (AB659224)
EH-Clone-3	KT864879	Cc, Hm, **Co**	Bacteroidetes	Uncultured Sphingobacteria bacterium clone LW18m-4-12 (EU640626)
EH-Clone-4	KT864880	Cc, **Hm**, Co	Actinobacteria	Uncultured bacterium clone LNH_9_9_11_Water.68898 (KM129052)
EH-Clone-5	KT864881	Cc, **Hm**, Co	Firmicutes	*Lactococcus* sp. JIP 26-01 (AM490370)
EH-Clone-6	KT864882	**Cc**	Cyanobacteria	*Calothrix* sp. HA4283-MV5 clone p11D (HQ847579)
EH-Clone-7	KT864883	**Tm**	Bacteroidetes	Agricultural soil bacterium clone SC-I-38 (AJ252632)
EH-Clone-8	KT864884	Hm, **Co**	Bacteroidetes	Uncultured bacterium clone LLEBRETA_A2 (HE857487)
EH-Clone-9	KT864885	Cc, **Hm**, Co	Alphaproteobacteria	Uncultured bacterium clone Ontario1224 (FJ390697)
EH-Clone-10	KT864886	Cc, **Hm**	Gammaproteobacteria	*Pseudomonas* sp. isolate NAF88 (AJ271413)
EH-Clone-11	KT864887	Cc, Hm, **Co**	Gammaproteobacteria	Uncultured *Acinetobacter* sp. clone BJS72-071 (AB238991)
EH-Clone-12	KT864888	**Cc**, Hm, Co	Bacteroidetes	Uncultured Flavobacteriaceae bacterium clone LW18m-2-34 (EU642386)
EH-Clone-13	KT864889	**Cc**, Co	Cyanobacteria	Uncultured bacterium clone BC12 (JX905999)
EH-Clone-14	KT864890	Cc, **Co**	Bacteroidetes	*Flavobacterium* sp. HME7802 (JN622005)
EH-Clone-15	KT864891	**Cc**	Cyanobacteria	Uncultured bacterium clone N06Jan-62 (GQ923920)
EH-Clone-16	KT864892	**Hm**	Alphaproteobacteria	Uncultured proteobacterium clone Gap-3-93 (EU639749)
EH-Clone-17	KT864893	**Cc**, Hm	Gammaproteobacteria	*Escherichia coli* (AF076037)
EH-Clone-18	KT864894	**Cc**	Gammaproteobacteria	Uncultured gamma proteobacterium clone wn56 (JQ012289)
EH-Clone-19	KT864895	Cc, Hm, **Co**	Bacteroidetes	*Gelidibacter gilvus* strain CL-2.1 (HQ113224)
EH-Clone-20	KT864896	Cc, **Hm**, Co	Betaproteobacteria	Uncultured bacterium clone B-27 (HQ860573)
EH-Clone-21	KT864897	Cc, **Co**	Bacteroidetes	*Chryseobacterium* sp. LDA39 G1966 12c (AY468468)
EH-Clone-22	KT864898	Cc, **Hm**	Alphaproteobacteria	Uncultured *Novosphingobium* sp. clone AV_4S-G07 (EU341160)
EH-Clone-23	KT864899	Cc, **Hm**, Co	Bacteroidetes	*Chryseobacterium* sp. LDA39 G1966 12c (AY468468)
EH-Clone-24	KT864900	Cc, **Hm**, Co	Bacteroidetes	Uncultured bacterium clone LLEBRETA_A2 (HE857487)
EH-Clone-25	KT864901	**Cc**, Hm	Bacteroidetes	Uncultured bacterium clone Filia_1_F1 (HE857129)
EH-Clone-26	KT864902	**Cc**, Hm, Co	Firmicutes	Uncultured bacterium isolate d21l12b27 (FR687152)
EH-Clone-27	KT864903	Cc, **Hm**, Co	Betaproteobacteria	Uncultured beta proteobacterium clone LiUU-3-218 (AY509424)
EH-Clone-28	KT864904	**Hm**, Co	Alphaproteobacteria	Uncultured bacterium clone UOXC-c02 (EU869719)
EH-Clone-29	KT864905	Cc, Hm, **Co**	Alphaproteobacteria	Uncultured bacterium clone DCBP.0912.138 (HQ904924)
EH-Clone-30	KT864906	**Cc**	Bacteroidetes	Uncultured bacterium clone S74 (JQ305080)
EH-Clone-31	KT864907	Cc, **Hm**, Co	Cyanobacteria	Uncultured cyanobacterium clone HG315 (FN646729)
EH-Clone-32	KT864908	Cc, **Hm**, Co	Alphaproteobacteria	Uncultured *Sphingopyxis* sp. clone5B_22 (HE861131)
EH-Clone-33	KT864909	**Cc**, Co	Cyanobacteria	Uncultured bacterium clone WH2 (GU981843)
EH-Clone-34	KT864910	**Hm**	Gammaproteobacteria	Uncultured *Acinetobacter* sp. clone BJS72-071 (AB238991)
EH-Clone-35	KT864911	**Cc**, Hm, Co	Cyanobacteria	Uncultured phototrophic eukaryote clone PM2-29 (EF215817)
EH-Clone-36	KT864912	Cc, **Hm**, Co	Cyanobacteria	Uncultured *Nostocales cyanobacterium* clone Cya35_Flocs (DQ804451)
EH-Clone-37	KT864913	Cc, **Hm**, Co	Alphaproteobacteria	Uncultured bacterium clone ORS10C_h01 (EF392934)
EH-Clone-38	KT864914	Cc, **Hm**, Co	Actinobacteria	Uncultured actinobacterium TH3-15 (AM690914)
EH-Clone-39	KT864915	Cc, **Hm**, Co	Alphaproteobacteria	Uncultured bacterium clone DROTU-07 (FJ546377)
EH-Clone-40	KT864916	Cc, **Hm**, Co	Bacteroidetes	Uncultured bacterium clone SGE25F (GU389983)
EH-Clone-41	KT864917	Cc, **Hm**, Co	Alphaproteobacteria	Uncultured bacterium clone WPUB150 (FJ006769)
EH-Clone-42	KT864918	Cc, **Hm**, Co	Bacteroidetes	Uncultured bacterium clone E5 (HQ853003)
EH-Clone-43	KT864919	Cc, **Hm**	Alphaproteobacteria	Uncultured *Sphingopyxis* sp. clone5B_22 (HE861131)
EH-Clone-44	KT864920	Cc, Hm, **Co**	Actinobacteria	Uncultured actinobacterium clone CB01B07 (EF471625)
EH-Clone-45	KT864921	**Hm**, Co	Betaproteobacteria	Uncultured bacterium clone 173ds20 (AY212624)
EH-Clone-46	KT864922	**Hm**	Alphaproteobacteria	Uncultured bacterium clone Ontario1224 (FJ390697)
EH-Clone-47	KT864923	Hm, **Co**	Actinobacteria	Uncultured bacterium clone YE201F11 (FJ694584)
EH-Clone-48	KT864924	Cc, Hm, **Co**	Actinobacteria	Uncultured actinobacterium clone CB01G05 (EF471487)
EH-Clone-49	KT864925	Cc, Hm, **Co**	Firmicutes	*Exiguobacterium* sp. WMF-7 (AM689995)
EH-Clone-50	KT864926	**Hm**	Alphaproteobacteria	Uncultured bacterium 28RHF13 (AJ863374)
EH-Clone-51	KT864927	Cc, **Hm**	Actinobacteria	Microbacteriaceae bacterium CNRB14 (GU300720)

[a] habitats in which this band occurred: Cc, Hm, and Co represents the three treatments *Cyprinus carpio*, *Hypophthalmichthys molitrix*, and control, respectively. Bold means the band is dominant in the group. The first band obtained from the top of region of the DGGE gels indicated by EH-Clone-1, the second band named EH-Clone-2. The other bands were named in the same manner.